Electronic Supplementary Material (ESI) for Nanoscale.
This journal is © The Royal Society of Chemistry 2022

Supplementary information

Regulating coordination capacity of ATMP by melamine: Facile synthesis of cobalt phosphides as bifunctional electrocatalysts for ORR and HER

Lian-Hua Xu[a,b], Wen-Ju Wang[c,**], Xue-Ji Zhang[a], Serge Cosnier[d], Robert S. Marks[e], Dan Shan[a,*]

[a] *MIIT Key Laboratory of Advanced Display Materials and Devices, School of Environmental and Biological Engineering, Nanjing University of Science and Technology, Nanjing 210094, China*

[b] *MOE Key Lab. of Environmental Remediation and Ecosystem Health, Institute of Environmental Health, College of Environmental and Resource Sciences, Zhejiang University, Hangzhou 310058, China*

[c] *School of Energy and Power Engineering, Nanjing University of Science and Technology, Nanjing 210094, China*

[d] *University of Grenoble Alpes-CNRS, DCM UMR 5250, F-38000 Grenoble, Francee*

[e] *Department of Biotechnology Engineering, Ben-Gurion University of the Negev, Beer-Sheva, Israel.*

*Corresponding author:

Email: danshan@njust.edu.cn (D. Shan)

wangwenju1982@gmail.com (W.J. Wang)

Fax: 0086-25-84303107

Contents

Figure S7 C_{dl} stands for ECSA of the three electrocatalysts for ORR.

Figure S8 The CV plots of **(A)** NCP, **(B)** HNCP and **(C)** N-CoP/NC with different scan rates in 0.5 M H_2SO_4 electrolyte.

Figure S9 EISs of NCP, HNCP and N-CoP/NC tested at 0.16 V vs. RHE.

Figure S10 (A) XRD and **(B)** HRTEM patterns of N-CoP/NC after ORR.

Figure S11 (A) XRD and **(B)** HRTEM patterns of N-CoP/NC after HER.

Materials characterization

The ultraviolet absorption spectrum of the specimens were measured by a liquid ultraviolet-visible spectrophotometer (UV-3600, Shimadzu Corporation). Their infrared spectrum was measured by TENSOR Model 27 Fourier Transform Infrared Spectrometer (FI-IR), while the Raman spectrum test was carried out with a Raman microscope (Raman, iHR550, HORIBA Scientific Instruments Division), using a 532 nm solid-state laser as the laser source, and the test range at 200-2000 cm^{-1}. The thermogravimetric-differential scanning calorimetry analysis of the sample was carried out on a synchronous thermal analyzer (TG-DSC, STA 449 F1 Jupiter, manufactured by Netzsch Instruments, Germany), the temperature range was taken from room temperature to 900 ^{o}C, the heating rate at 10 ^{o}C/min; The crystal phase of the samples was characterized by X-ray diffraction (XRD, Bruker D8, Bruker Technology Co., Ltd.) with a power of 40 kV/40 mA. The scanning range was set at 10-60^{o}; The BET results were recorded on Quantachrome Autosorb-iQ-C.The morphology and size of the synthetate was visualized using a transmission electron microscope (TEM, FEI Tecnai 20, FEI company in the United States) and a high resolution transmission electron microscope (HRTEM, Jeol jem2100f, Japan Electronics (JEOL) company). The crystal structure and element morphology of the specimens were characterized by X-ray photoelectron spectroscopy (XPS, ESCALAB 250XI, Thermo Fisher Scientific, Germany). All spectra used the binding energy of C 1s peak at 284.6 eV Calibration.

Electrochemical measurements

A three-electrode cell was operated for electrochemical analysis for all the aforementioned catalysts. A graphite rod was used as a counter electrode, Hg/HgO and Hg/Hg_2SO_4 electrode were used as reference electrodes for ORR and HER test respectively. To prepare the catalyst ink, 10.0 mg of catalyst was dispersed into 0.25 mL of ethanol and 0.75 mL of DI water, and then sonicated for 30 mins to obtain a homogeneous slurry. To prepare a working electrode, 10 μL of the slurry was dropped on a rotating disk electrode (diameter 5 mm, RDE, Metrohm) for ORR or a polished glass carbon (GC) electrode for OER and both, dried slowly under ambient conditions. A commercial Pt/C electrode (20 wt%) was also prepared for the comparison tests. All catalyst loading was controlled at 0.51 mg cm^{-2}. For ORR, the performance was first recorded by cyclic voltammetry (CV) in O_2-saturated 0.1 mol L^{-1} KOH with a scan rate of 10 mV s^{-1} at room temperature. Linear scanning voltammetry (LSV) was performed in a potential range from 0.2 to -0.8 V with different rotation rates (400, 625, 900, 1225, 1600 and 2025 rpm) at a scan rate of 10 mV s^{-1}. During testing, a constant injection of O_2 or N_2 was maintained in the electrolyte. All the potentials were converted to a reversible hydrogen electrode (RHE), E (RHE) = E (Hg/Hg_2Cl_2) + 1.008 V. The HER performance was collected in an N_2 saturated 0.5 M H_2SO_4 solution. E (RHE) = E (Hg/Hg_2Cl_2) + 0.240 V.

Calculation methods

All DFT calculations were recorded as implemented in the Vienna *Ab Initio* Simulation Package (VASP),[1, 2] so as to describe the interaction between the electrons with frozen-core approximation and ions. Furthermore, the projector augmented wave (PAW) method with the Perdew-Burke-Ernzerhof (PBE) was performed.[3] Until the forces acting on each ion reached a smaller value than 0.05 eV/Å, the stationary points were identified by the conjugate gradient method. The k-points meshes of 1 × 1 ×1 were collected for the Brillouim zone integration. The convergence tolerance of the energy was set to be 10^{-4} eV.

The two opposite reaction pathways of ORR (1-4) can be expressed as the following steps [4]:

$$O_2 + * + (H_2O\,(l) + e^-) \rightarrow OOH^* + OH^- \quad (1)$$

$$OOH^* + e^- \rightarrow O^* + OH^- \quad (2)$$

$$O^* + (H_2O\,(l) + e^-) \rightarrow OH^* + OH^- \quad (3)$$

$$OH^* + e^- \rightarrow OH^- + * \quad (4)$$

Here * represents an active site on the catalysts surface, whereas, OH*, O*, OOH* represent catalytic intermediates. The free energies were collected using Eq. (9).[5] In the following, T (298.15 K) represents temperature, ΔZPE the change of zero-point energy, and ΔS the difference in entropy. $\Delta G_U = -neU$, where U is the potential of the electrode and n is the number of electrons transferred. $\Delta G_{pH} = K_B T \times \ln 10 \times pH$, where

K_B is the Boltzmann constant, the pH value for ORR was defined to be 14, for OER was 14, for HER was 0.

$$\Delta G = \Delta E + \Delta \mathrm{ZPE} - T\Delta S + \Delta G_U + \Delta G_{PH} \quad (5)$$

For HER, the Gibbs free energy of H adsorption was obtained by Eq. (10)

$$\Delta G_H = \Delta E_H + \Delta E_{ZPE} - T\Delta S_H \quad (6)$$

Where ΔE_{ZPE} is the zero-point energy and ΔS_H is the entropy. $\Delta E_{ZPE} - T\Delta S_H$ is 0.28 eV in standard condition at $T = 300$ K.

Therefore, the ΔG_H was calculated by Eq. (11)

$$\Delta G_H = \Delta E_H + 0.28\ \mathrm{eV} \quad (7)$$

Table S1 BET results of NCP, HNCP and N-CoP/NC.

Catalysts	specific surface area ($m^2\ g^{-1}$)	pore volume ($cm^3\ g^{-1}$)
NCP	159	0.252
HNCP	271	0.532
N-CoP/NC	427	0.627

Table S2 Quantitative XPS analysis for N-CoP/NC, HNCP and NCP.

Element	Peak	N-CoP/NC		HNCP		NCP	
		Position (eV)	Content (%)	Position (eV)	Content (eV)	Position (eV)	Content (eV)
Co 2p	**Co_{total}**	-	2.07	-	-	-	-
	Co-P	779.53	17.31	-	-	-	-
	Co-POx	781.78	49.64	-	-	-	-
	Sat.	786.18	33.05				
N 1s	**N_{total}**	-	4.71	-	5.93	-	4.72
	Pyridinic N	398.42	12.25	398.73	13.09	398.62	13.04
	Pyrrolic N	-	-	399.40	23.03	400.22	24.65
	Co-N	399.59	24.91	-	-	-	-
	Graphitic N	401.17	61.69	401.23	61.65	401.53	35.84
	Oxidated N	403.70	1.15	404.04	2.23	402.86	26.46
P 2p	**P_{total}**	-	7.75	-	6.87	-	8.82
	$2P_{3/2}$	129.83	10.21	-	-	-	-
	$2P_{1/2}$	130.56	5.25	-	-	-	-
	POx	133.6	84.54	133.45	100.00	134.35	100.00
O 1s	**O_{total}**		12.16		19.28		36.37
	-O-	530.56	27.53	530.55	32.67	530.66	20.85
	-OH/O_2	531.54	21.09	531.52	34.67	531.81	43.16
	H_2O	532.74	51.38	532.58	32.66	533.00	35.98

Figure S1

Figure S2

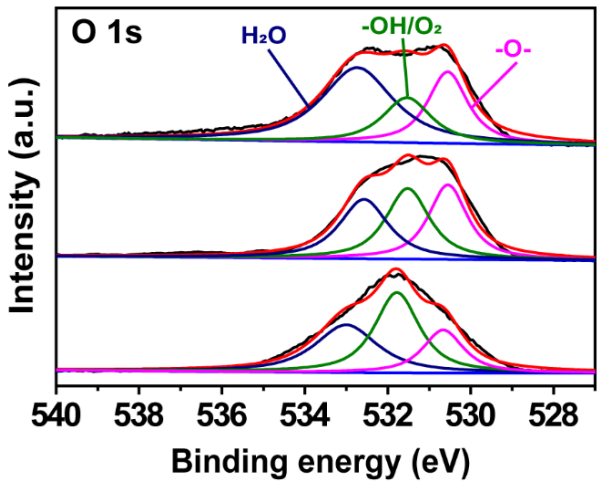

Figure S3

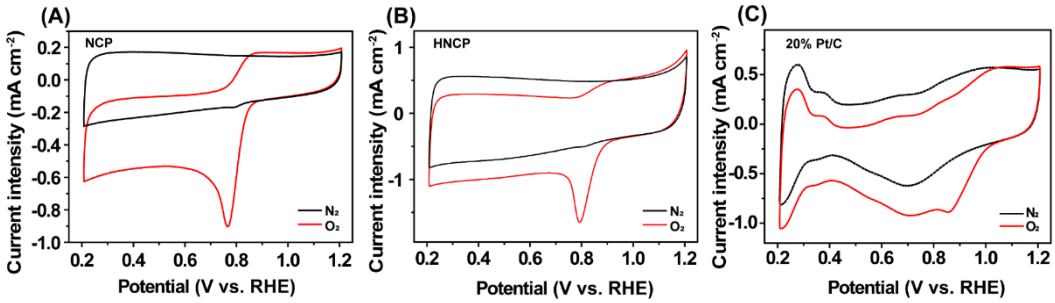

Figure S4

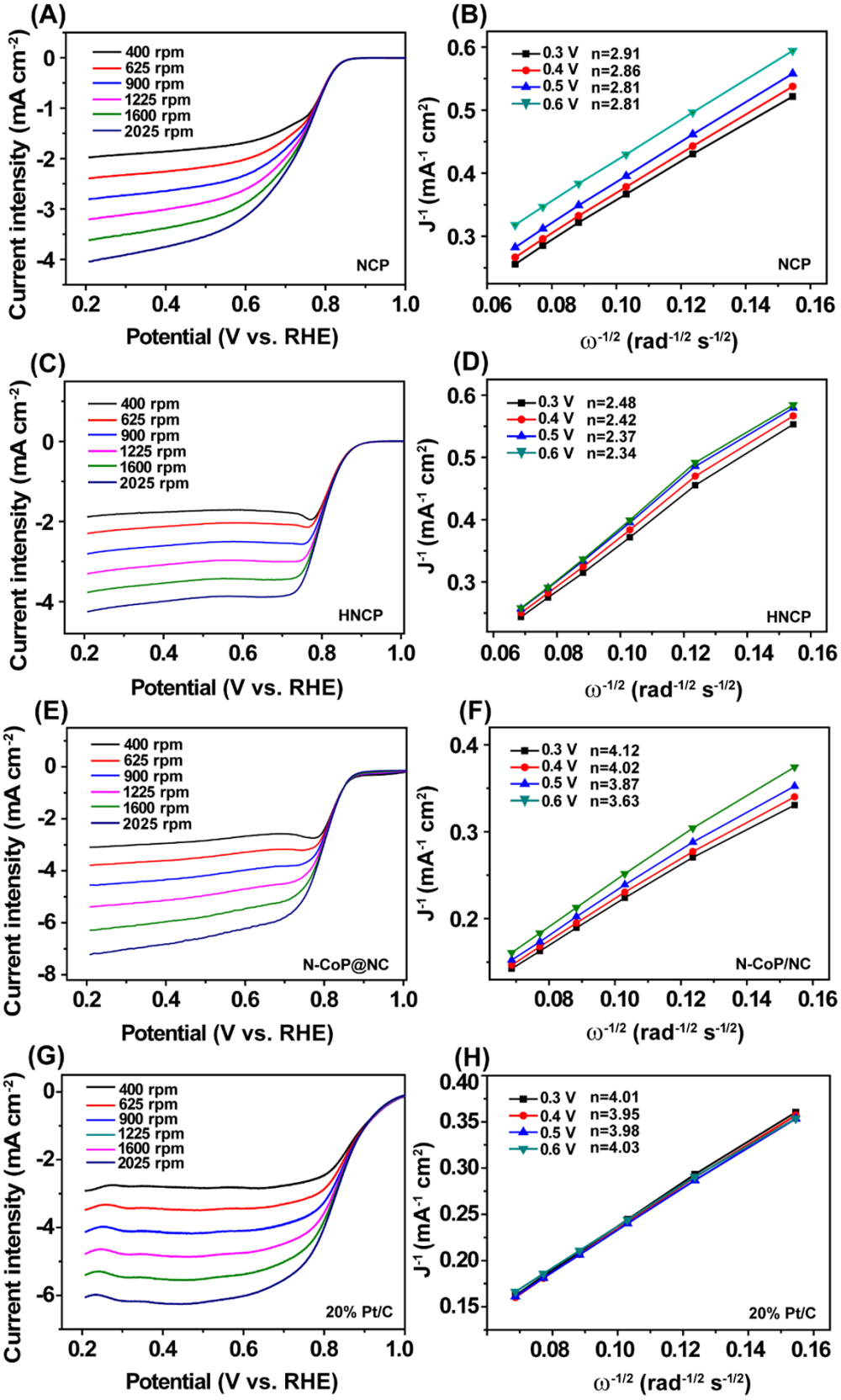
(A)
Current intensity (mA cm-2)
400 rpm
625 rpm
900 rpm
1225 rpm
1600 rpm
2025 rpm
NCP
Potential (V vs. RHE)
(B)
0.3 V n=2.91
0.4 V n=2.86
0.5 V n=2.81
0.6 V n=2.81
NCP
J-1 (mA-1 cm2)
ω-1/2 (rad-1/2 s-1/2)
(C)
HNCP
(D)
0.3 V n=2.48
0.4 V n=2.42
0.5 V n=2.37
0.6 V n=2.34
HNCP
(E)
N-CoP@NC
(F)
0.3 V n=4.12
0.4 V n=4.02
0.5 V n=3.87
0.6 V n=3.63
N-CoP/NC
(G)
20% Pt/C
(H)
0.3 V n=4.01
0.4 V n=3.95
0.5 V n=3.98
0.6 V n=4.03
20% Pt/C

Figure S5

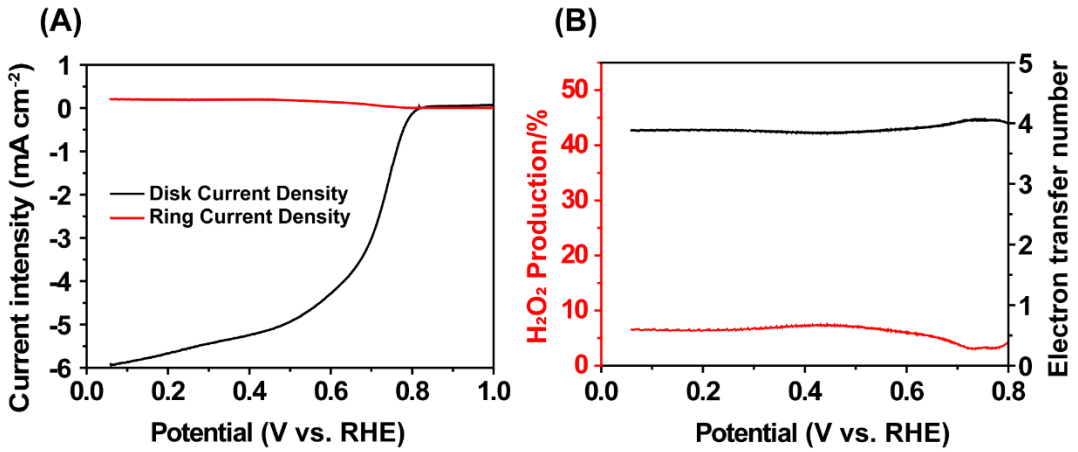

Figure S6

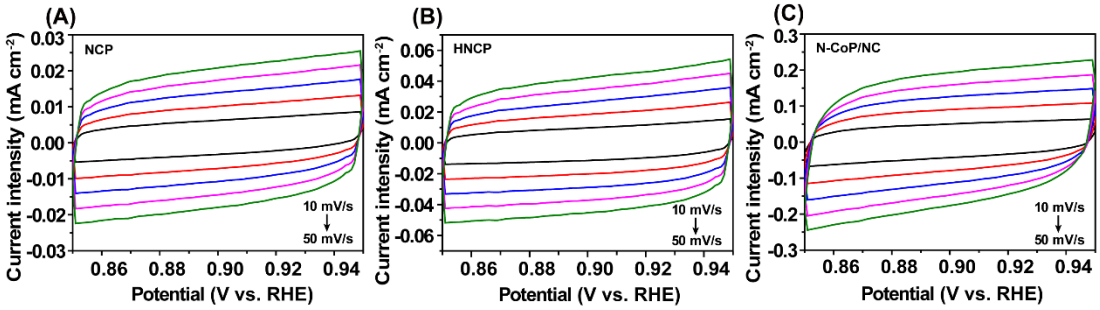

Figure S7

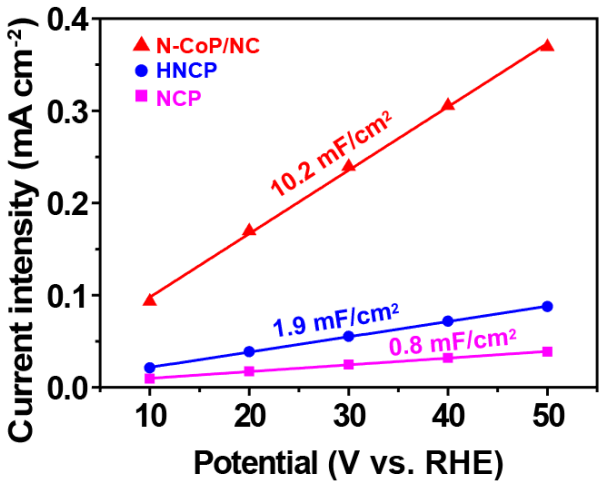

Figure S8

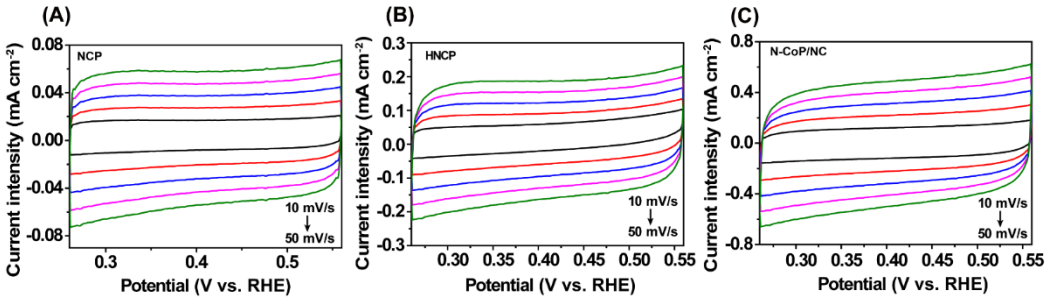

Figure S9

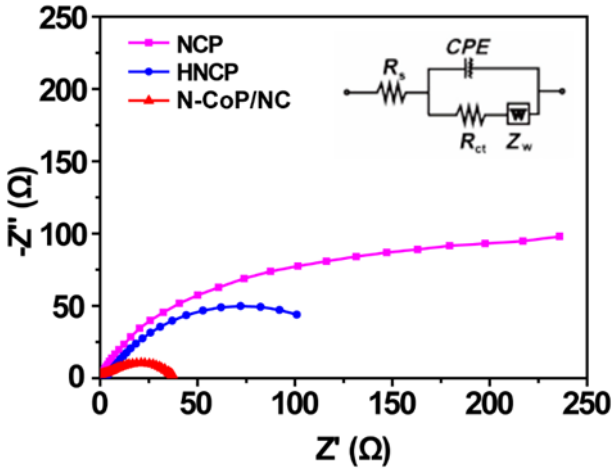

Figure S10

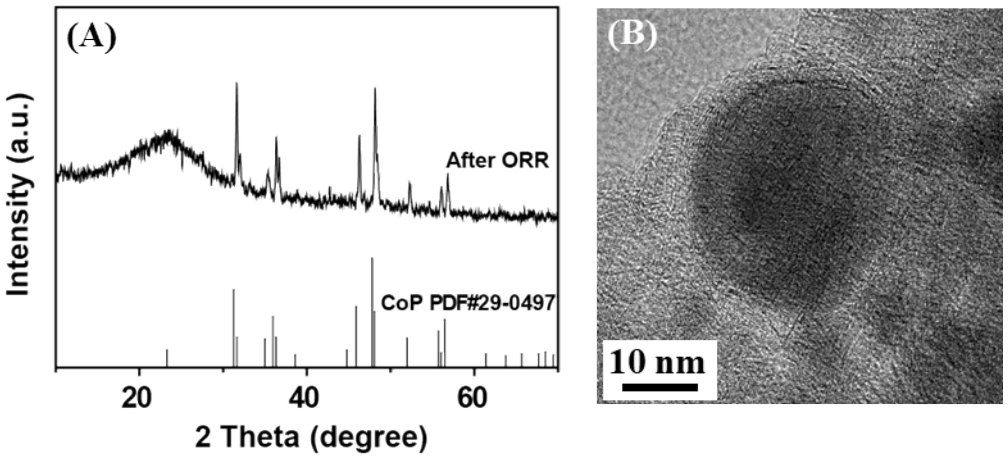

Figure S11

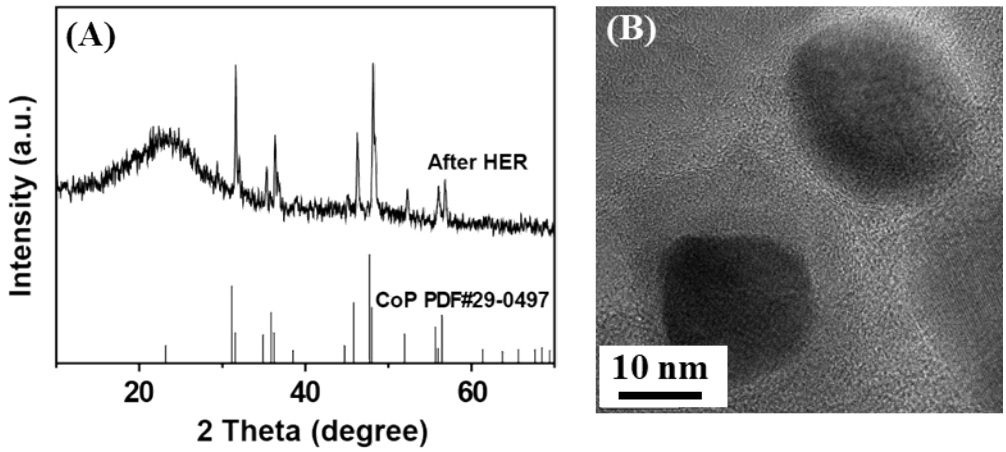
(A)
Intensity (a.u.)
After HER
CoP PDF#29-0497
20
40
60
2 Theta (degree)
(B)
10 nm

Table S3 Comparison of ORR performance of some recently reported TMPs and doped CoP electrocatalysts in 0.1 M KOH.

Catalyst	E_{onset} (V vs. RHE)	$E_{1/2}$ (V vs. RHE)	j_{limit} (mA/cm^2)	Ref.
Our work	**0.908**	**0.824**	**6.280**	**This work**
CoP/NC-800	0.90	0.78	4.60	[6]
Co_2P/CoN-in-NCNTs	0.96	0.85	5.01	[7]
Co_2P@NPC-1	-	0.83	5.12	[8]
CoP-PBSCF	-	0.75	~4.60	[9]
CoP	-	0.62	-	[9]
Bi-CoP/NP-DG	-	0.81	-	[10]
CoNP@NC/NG	0.90	0.83	4.55	[11]
CoP@SNC	0.87	0.79	~4.85	[12]
Co_2P@CoNPG-800	0.90	0.81	-	[13]
Fe/Co-NpGr	0.93	N.A.	~4.25	[14]
Co/CoP-HNC	-	0.83	~4.95	[15]
CoP/Ni_2P@NC/NF	-	0.79	4.95	[16]
CoP/CN/Ni	-	0.80		[17]
FeCo/Co_2P@NPCF	0.825	0.78		[18]

Table S4 Comparison of HER performance of some other TMPs and doped CoP electrocatalysts in 0.5 M H_2SO_4.

Catalyst	η_{10} (mV)	Tafel slope (mV dec^{-1})	Ref.
Our work	150	77	This work
CoP/HNCNP@2DCoP	173	108.7	[19]
CoP/HNCNP	189.5	168.5	[19]
amorphous CoP/NF	143	-	[20]
HNDCM-Co/CoP	216	-	[21]
Co_2P NR/Ti	134	-	[22]
CoP NBA/Ti	203		[23]
$Ni_{0.62}Co_{0.38}P$	166	72	[24]
CoP@NC	170	62	[25]
$Co_5Mo_{1.0}P$ NSs@NF	174	190	[26]
CoP/RGO	157	70.2	[27]
CoP/Co_2P/Co	169	65	[28]
CoP microspheres	226	76	[29]
CoP/CNTs	198	68	[30]

References:

1. G. Kresse and J. Hafner, Phys. Rev. B, 47 1993, 47, 558.
2. G. Kresse and J. Hafner, Phys. Rev. B, 1994, 49, 14251.
3. P.E. Blöchl, Phys. Rev. B, 1994, 50, 17953.
4. Z. Zhao and Z. Xia, ACS Catal. 2016, 6, 1553-1558.
5. M. Ma, A. Kumar, D. Wang, Y. Wang, Y. Jia, Y. Zhang, G. Zhang, Z. Yan and X. Sun, Appl. Catal., B, 2020, 274, 119091.
6. L. Feng, R. Ding, Y. Chen, J. Wang and L. Xu, J. Power Sources, 2020, 452, 227837.
7. Y. Guo, P. Yuan, J. Zhang, H. Xia, F. Cheng, M. Zhou, J. Li, Y. Qiao, S. Mu and Q. Xu, Adv. Funct. Mater., 2018, 28, 1805641.
8. J. Li, G. Liu, B. Liu, Z. Min, D. Qian, J. Jiang and J. Li, Int. J. Hydrogen Energy, 2018, 43, 1365-1374.
9. Y. Q. Zhang, H. B. Tao, Z. Chen, M. Li, Y. F. Sun, B. Hua and J. L. Luo, J. Mater. Chem. A, 2019, 7, 26607-266017.
10. Z. Chen, H. Wu, W. Guo, C. Cao and Z. Chen, Appl. Catal., B, 2019, 265, 118576.
11. X. Zhong, Y. Jiang, X. Chen, L. Wang, G. Zhuang, X. Li and J. G. Wang, J. Mater. Chem. A, 2016, 4, 10575-10584.
12. T. Meng, Y. N. Hao, L. Zheng and M. Cao, Nanoscale 2018, 10, 14613-14626.
13. H. Jiang, C. Li, H. Shen, Y. Liu, W. Li and J. Li, Electrochim. Acta, 2017, 231, 344-353.

14. T. Palaniselvam, V. Kashyap, S. N. Bhange, J. B. Baek and S. Kurungot, Adv. Funct. Mater., 2016, 26, 2150-2162.
15. Y. Hao, Y. Xu, W. Liu and X. Sun, Mater. Horiz., 2018, 5, 108-115.
16. X. Lv, W. Tian, Y. Liu and Z. Y. Yuan, Mater. Chem. Front., 2019, 3, 2428-2436.
17. T. Chen, J. Ma, S. Chen, Y. Wei, C. Deng, J. Chen, J. Hu and W. Ding, Chem. Eng. J., 2021, **415**, 129031.
18. Q. Shi, Q. Liu, Y. Ma, Z. Fang, Z. Liang, G. Shao, B. Tang, W. Yang, L. Qin and X. Fang, Adv. Energy Mater. 2020, **10**, 1903854.
19. S. Lv, J. Chen, X. Chen, J. Chen and Y. Li, ChemSusChem, 2020, 13, 3495-3530.
20. R. Beltrán-Suito, P. W. Menezes and M. Driess, J. Mater. Chem. A, 2019, 7, 15749-15756.
21. H. Wang, S. Min, Q. Wang, D. Li, G. Casillas, C. Ma, Y. Li, Z. Liu, L. J. Li, J. Yuan, M. Antonietti and T. Wu, ACS Nano, 2017, 11, 4358-4364.
22. Z. Huang, Z. Chen, Z. Chen, C. Lv, M.G. Humphrey and C. Zhang, Nano Energy, 2014, 9, 373-382.
23. Z. Niu, J. Jiang and L. Ai, Electrochem. Commun., 2015, 56, 56-60.
24. J. Yu, Q. Li, Y. Li, C. Y. Xu, L. Zhen, V. P. Dravid and J. Wu, Adv. Funct. Mater., 2016, 26, 7644-7651.
25. S. Gao, Y. Liu, G. D. Li, Y. Guo, Y. Zou and X. Zou, Electrochim. Acta, 2016, 199, 99-107.
26. Y. Zhang, Q. Shao, S. Long and X. Huang, Nano Energy, 2018, 45, 448-455.
27. Y. You, W. Zeng, Y. X. Yin, J. Zhang, C. P. Yang, Y. Zhu and Y. G. Guo, J.

Mater. Chem. A, 2015, 3, 4799-4802.

28. A. Sumboja, T. An, H. Y. Goh, M. Lübke, D. P. Howard, Y. Xu, A. D. Handoko, Y. Zong and Z. Liu, ACS Appl. Mater. Inter., 2018, 10, 15673-15680.
29. Q. Liu, J. Tian, W. Cui, P. Jiang, N. Cheng, A. M. Asiri and X. Sun, Angew. Chem. Int. Ed., 2014, 53, 1-6.
30. Y. Pan, Y. Lin, Y. Chen, Y. Liu and C. Liu, J. Mater. Chem. A, 2016, 13, 4745-4754.